Influence of Fluorine Substitution on the Proton Conductivity of Hydroxyapatite

By **Gobinda C. Maiti** and **Friedemann Freund,*** Mineralogisch-Petrographisches Institut, Universität zu Köln, Zülpicher Straße 49, D–5000 Köln–1, Federal Republic of Germany

Polycrystalline hydroxyfluoro-apatite solid solutions exhibit pronounced proton conductivity, $\sigma(H^+)$, in the range 250—500 °C. For samples with between 0 and 50% F the activation energy for $\sigma(H^+)$ remains constant, 0.6 (±0.1) eV, but rises sharply for samples with 65 (1.1 eV), 75 (1.3 eV), and for *ca.* 100% F (1.4 eV). The frequency factor, σ_0, increases with increasing F content up to 50% F, but drops sharply for higher percentages of F substitution. The dominant protonic charge carriers are defect protons as deduced from thermopotential measurements.

In the apatite structure, $Ca_5(PO_4)_3X$, the X^- ions (X = OH, F, or Cl) form one-dimensional chains parallel to the *c* axis.[1-4] The X–X distance is large, typically 3.44 Å for OH^- and F^- in apatite.[1,5,6] This suggests that, for hydroxyapatite, no hydrogen-bond type interaction exists between adjacent OH^-, as evidenced by the single narrow ν(OH) stretching band at 3 573 cm^{-1} in the i.r. spectrum of pure stoicheiometric hydroxyapatite.[7,8] Incorporation of F^- into the one-dimensional OH^- chain leads to a shift and broadening of this i.r. band and to the appearance of a new ν(OH) band at 3 540 cm^{-1} which persists up to *ca.* 100% F^-.[9,10] This band, displaced by 33 cm^{-1} to lower frequencies, is due to the O–H stretching vibration of a single hydroxide ion dispersed in an F^- chain. The small amount of this displacement indicates that the H-bond type interaction, $OH^- \cdots F^-$, remains weak.[11,12] This statement is supported by the fact that the mean OH–F distance, as deduced from the c_0 parameter of the unit cell of (OH, F) apatite solid solutions, remains essentially constant. Furthermore, it can be concluded from the i.r. results, in particular from the sharpness of the ν(OH) stretching band in hydroxyapatite, that the interaction between the OH^- and the PO_4^{3-} groups of the calcium phosphate sublattice is essentially ionic with little or no indication of H-bond type bonding.

Ionic diffusion along the *c* axis of apatites has been studied by various authors.[13-15] Proton conductivity measurements, however, seem not to have been attempted until now. Recent advances in the understanding of proton conductivity behaviour of simple ionic hydroxides [16-19] led to the expectation that hydroxyapatite and (OH, F)apatite solid solutions might exhibit an interesting proton conductivity behaviour.

Furthermore, proton transport along the OH^- chain in apatite is probably the elementary step in the acid attack which initiates demineralisation [20-22] and eventually leads to caries lesions. In this respect a study of the proton conductivity of hydroxyapatite and (OH, F)apatite solid solutions may provide important information regarding the mechanism by which F^- acts as a barrier to the acid attack.

EXPERIMENTAL

Samples and Measuring Technique.—Apatite powder samples were prepared by solid-state reaction from $Ca[HPO_4]\cdot 2H_2O$, $Ca[O_2CMe]_2$, and CaF_2 reaction grade chemicals. The chemicals were thoroughly mixed as acetone slurries by mechanical stirring for 1 h. The mixtures were dried, pelletised, and heated in an open platinum crucible to 1 000 °C for 10 h in a stream of decarbonated moist air (P_{H_2O} = 4 Torr †). The samples were cooled slowly, crushed, and powdered in an agate ball mill. The heating and homogenisation cycles were repeated three times in a stream of moist air in order to complete the reaction and prevent dehydroxylation.

The apparatus for the proton conductivity and thermopotential measurements is shown in Figure 1. It consists

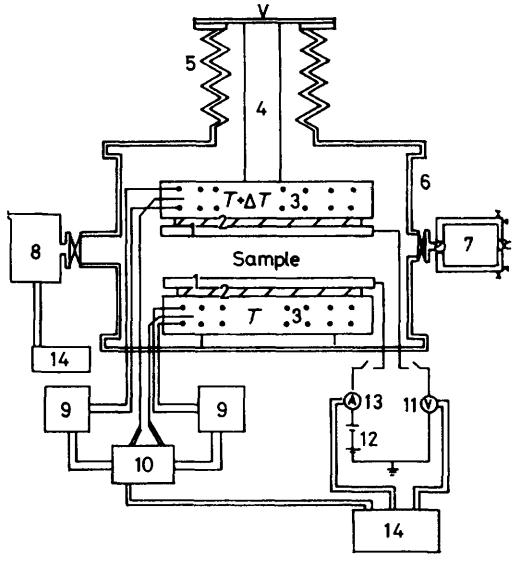

FIGURE 1 Block diagram and sample chamber for the measurement of d.c. currents and thermopotentials. Gold electrodes (1), BeO insulators (2), stainless steel furnaces with coaxial heaters (3), alumina ceramic tube (4), flexible connector tubing (5), recipient, internally nickel plated (6), carrier gas inlet and H_2 gas loop (7), gas chromatograph (8), separate temperature controllers (9), temperature programmers (10), electrometer (11), high voltage supply (12), pico-amperemeter (13), recorders (14)

of two separately heated stainless steel furnace blocks (50 × 60 × 15 mm). Shielded coaxial Nichrome wires were used as heaters. The two furnaces were set at T and $T + \Delta T$ by means of two separate temperature controllers. ΔT was of the order of 10—15 K depending on the temper-

† Throughout this paper: 1 Torr = (101 325/760) Pa, 1 eV ≈ 1.60×10^{-19} J; 1 bar = 10^5 Pa.

ature range and was measured by two Chromel-Alumel thermocouples in differential. All wires carrying the signal were made out of electrolyte copper and shielded against stray fields. The electrode consisted of thin palladium sheets, 0.1 mm, on which palladium black was chemically deposited from an aqueous $PdCl_2$ solution (1 mol dm^{-3}). The electrodes were then saturated with H_2. The electrodes were insulated from the furnace blocks by means of ceramic BeO, 1 × 40 mm ϕ (circular diameter), in addition to mica sheets (0.2 mm). A Keithley model 610 electrometer and a Keithley 480 pico-amperemeter were used for the thermopotential and d.c. conductivity measurements respectively.

The furnace temperature near the ceramic BeO and the current or, in separate runs, the furnace temperature and the thermopotential were registered simultaneously. The fast rise and exponential decay of the partial pressure of H_2 in the recipient was monitored by gas chromatography. The temperature near the ceramic BeO and, hence, near the electrode and the sample, showed no measurable change upon H_2 admission.

The apatite powder was pressed to thin pellets, 30 mm ϕ, with a pressure of 20 kg cm^{-2}. The pellet thickness was of the order of 0.1 mm. The applied voltage was 100 V, corresponding to 10^4 V cm^{-1} across the sample. The voltage was maintained at a constant value by a voltage stabiliser. Prior to each run, the samples were dried at 120 °C under an N_2 atmosphere (1 bar) for a sufficiently long time to establish a constant value of the current. The N_2 carrier gas (6 l h^{-1}) and the H_2 gas were dried over a molecular sieve. The palladium black electrodes were replaced after about 10 heating and pulse cycles. For reasons to be explained below the H_2 pulse technique was used (25 cm^3 H_2 pulses in 6 l h^{-1} N_2 flow). The desorption of H_2 pulses from the sample during flushing with N_2 was measured by means of a Dani 3 200 gas chromatograph equipped with a 2-m molecular sieve column.

Sample Characterisation.—All samples were characterised by chemical analysis for F (by F-sensitive LaF_3 electrode), Ca and P (by *X*-ray fluorescence), and by *X*-ray diffraction and i.r. spectroscopy. The compositions of the seven samples analysed are given in the Table.

Chemical analysis of (OH_{1-x},F_x)apatite

F(%)	x	Ca (%)	P (%)
0	0	39.4	18.4
0.57	0.15	39.5	18.3
1.31	0.35	39.6	18.2
1.89	0.50	39.6	18.3
2.41	0.64	39.4	18.4
2.79	0.74	39.5	18.3
3.61	0.96	39.4	18.4

The *X*-ray diffraction results indicate a single-phase apatite lattice with traces of CaO ($\lesssim 1\%$) detectable in some of the samples. The unit-cell parameters were determined by means of a Guinier double radius camera using monochromatic Cu-$K_{\alpha 1}$ radiation and least-squares refinement. The values for a_0 and c_0 are given in Figure 2.

The i.r. results, described in detail earlier,[10,23] indicated the formation of single-phase (OH, F)apatite solid solutions. The integrated i.r. intensities of the OH stretching and bending vibrations of the pure hydroxyapatite sample were equal or greater than those of hydroxyapatite samples precipitated from aqueous solution under a variety of experimental conditions. This clearly shows that no dehydroxylation was induced by the high-temperature sample preparation in steam described above. There was no indication of the formation of oxyapatite [24,25] for the mixed apatite samples used in the present study.

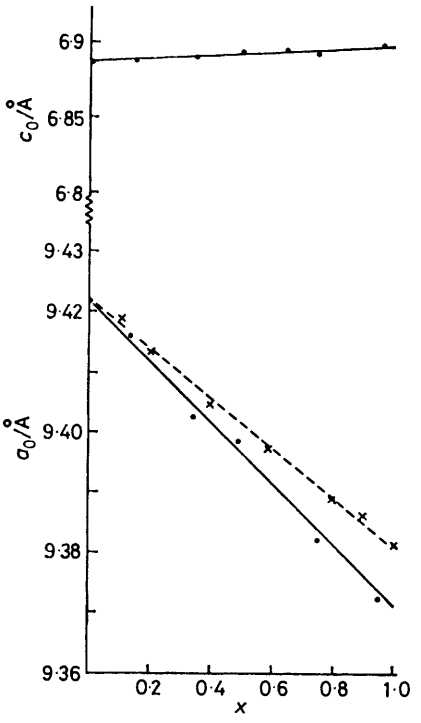

FIGURE 2 Variation of the lattice parameters of $Ca_5(PO_4)_3(OH)_{1-x}F_x$ (values marked with crosses are from E. C. Moreno, M. Kresak, and R. T. Zahradnik, *Caries Res. Suppl.*, 1977, **11**, 142)

RESULTS

As in the case of simple ionic hydroxides reported earlier,[16-19] the existence of proton conductivity was double checked (*a*) by carrying out measurements in H_2 or a H_2/N_2 gas mixture with either Au or Pd electrodes, or (*b*) by carrying out the same measurements with Pd electrodes and changing the N_2 atmosphere to H_2. In case (*a*) a more than 10-fold current increase was observed with Pd electrodes over Au electrodes. In case (*b*) the current increase on changing from N_2 to H_2 was up to eight-fold. Both measurements confirm the existence of an overwhelming protonic contribution to the conductivity under the appropriate conditions of H^+-injecting Pd electrodes in an H_2 atmosphere. In pure H_2 (1 bar), difficulties were encountered as a result of electrode polarisation due to oversaturation of the Pd with H_2. For this reason we used the H_2 pulse technique applied successfully in an earlier study.[26]

A typical current against time curve is shown in Figure 3. On applying the H_2 pulse, a very sharp increase in the current was observed followed by an equally rapid decrease to a value which was even lower than the starting value due to electrode polarisation. As the 6 l h^{-1} N_2 stream swept the H_2 pulse out of the sample chamber, the current rose once more, remained constant for some time, and then decayed exponentially. At the same time the H_2 gas in the sample chamber seemed to be swept out faster than before in spite of the constant flow of N_2. This is due to H_2

desorption from the Pd electrodes below a certain H_2 partial pressure.[26]

The conductivities shown in Figure 3 were reproducible with samples of different thickness in spite of the fact that the conductivity measurements were carried out with compressed powder pellets. This confirms the earlier observation [16,17] that these proton conductivity measurements seem not to be very sensitive to grain-to-grain contacts. Samples of different OH : F ratio differed in the

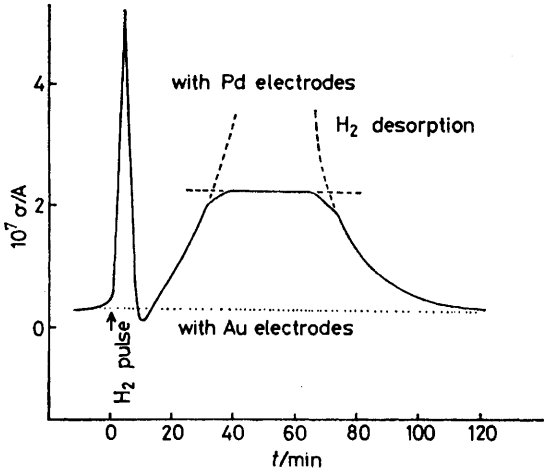

FIGURE 3 Type of d.c. conductivity, at 450 °C, as a function of time following an H_2 pulse on hydroxyapatite

height of the first sharp current peak and in the height of the current plateau, but not in the general shape of the current against time curve.

By plotting selected conductivity values on a logarithmic scale against T^{-1} (Arrhenius plot) straight lines are obtained

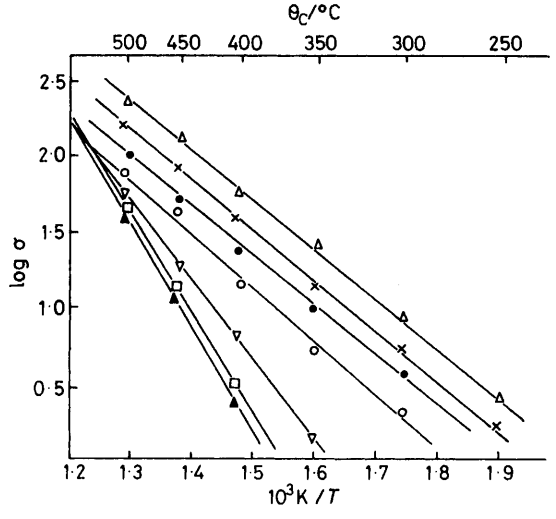

FIGURE 4 Arrhenius plot for the d.c. conductivity of (OH_{1-x},F_x)-apatites using the first maximum in the conductivity curves. x = 0.0 (○), 0.15 (●), 0.35 (×), 0.50 (△), 0.64 (▽), 0.74 (□), 0.96 (▲)

for all samples over the temperature range investigated. The Arrhenius plots derived from the values of the first sharp current peak are shown in Figure 4 and those from the plateau in Figure 5.

The protonic thermopotential measured simultaneously also gave a characteristic curve as shown in Figure 6. Under N_2 the sign of the thermopotential was consistently positive but changed to the negative direction upon the admission of H_2. The slightly p-type value persisted until

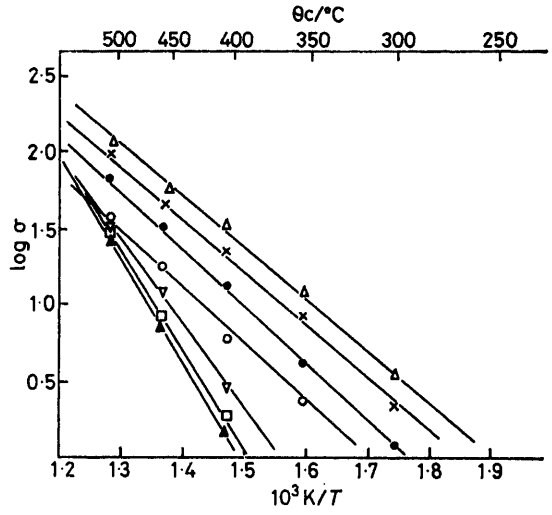

FIGURE 5 As Figure 4 but using the second maximum (the plateau) in the conductivity curve (symbols as in Figure 4)

the end of the current plateau. When the current started to decay exponentially, an irregularity was observed as reported earlier from other systems.[26] This irregularity is linked to the desorption of H_2 from the Pd electrodes. Thereafter the potential slowly returned to the initial value. With Au electrodes H_2 pulses gave no noticeable effect.

The characteristic changes in the thermopotential curves during and after an H_2 pulse reported here for the (OH, F)-apatite samples resemble in certain aspects the results obtained for γ-Al_2O_3 and Pt–γ-Al_2O_3 catalysts.[26]

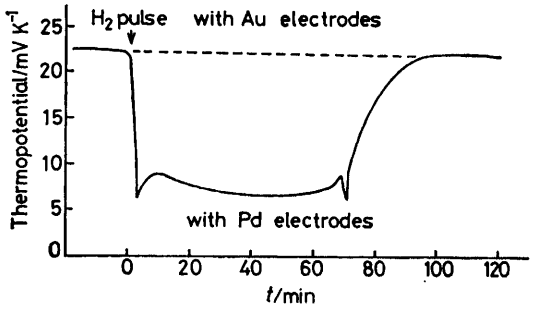

FIGURE 6 Type of thermopotential, at 450 °C, as a function of time following an H_2 pulse on hydroxyapatite

Even though the thickness of the powder samples in different runs was certainly subject to some slight variations, it was possible to reproduce the conductivity values of the (OH, F)apatite samples within narrow limits and to show that with increasing F substitution the currents increase in a systematic manner up to 50% F. At 65 and 75% F substitution and in the nearly pure fluoro-apatite, the currents obtained are definitely lower and characterised by different slopes in the Arrhenius plots.

DISCUSSION

Proton Band Model.—In hydroxyl groups which are essentially ionic (large OH · · · OH distances) the protons are tightly bound to their O^{2-} ions and therefore strictly localized within the electron cloud of O^{2-}. In order to remove a proton from this bound state special conditions are needed. The experimental results clearly indicate that proton conductivity does occur in (OH, F)apatite samples and that it is related to the F content.

The potential-energy curve of the hydroxyl protons along the linear OH · · · OH · · · OH chain (OH–OH distance, 3.4 Å) is not known in detail. From our work on ionic hydroxides [16-19] with similar OH–OH distances (*e.g.* 3.2 Å in $Mg[OH]_2$) we can deduce that the energy barriers separating neighbouring proton sites in hydroxyapatite are likely to be high (>2 eV).

The presence of nearby PO_4^{3-} ions probably modifies the potential-energy curve of the hydroxyl protons as evidenced by the shift of the O–H stretching frequency from typically 3 655 cm^{-1} in $Ca[OH]_2$ to 3 540—3 573 cm^{-1} in $Ca_5(OH, F)(PO_4)_3$ depending upon the F content.[10] However, the O–H stretching band in the i.r. spectrum of hydroxyapatite still remains rather narrow indicating little or no H-bond type interaction between OH^- and PO_4^{3-}.

In cases like $Al[OH]_3$, $Mg[OH]_2$, and $Ca[OH]_2$ one particular conductivity mechanism has been observed which points at proton transport *via* the delocalised state 1.65, 2.0, and 2.2 eV respectively above the zero-energy level.[16-19] This conductivity mechanism has been termed excess proton conductivity. The symbol H· is used to designate a proton in excess. The species H· is characterised by a high mobility and by the fact that it carries a net positive charge along a given OH^- array.

A second mechanism has been observed which can best be described as defect proton mechanism. A defect proton is essentially an isolated O^{2-} ion in a OH^- array, formed by a dissociation process according to equation (1). The species HOH is *not* a ' water ' molecule but the

$$OH^- + OH^- \rightleftharpoons O^{2-} + HOH \qquad (1)$$

transitory state H·. We can now apply this knowledge to the one-dimensional OH^- chain in the apatite structure.

If an H· forms somewhere and diffuses away along the OH^- chain or is trapped by some phosphate group, we are left with a defect proton in the OH^- chain which in turn can migrate *via* a proton exchange with neighbouring OH^- groups, for instance from left to right, see below. If the defect proton moves as shown here, a

O^{2-}	OH^-	OH^-	OH^-	OH^-	OH^-	OH^-
OH^-	O^{2-}	OH^-	OH^-	OH^-	OH^-	OH^-
OH^-	OH^-	O^{2-}	OH^-	OH^-	OH^-	OH^-
OH^-	OH^-	OH^-	O^{2-}	OH^-	OH^-	OH^-
OH^-	OH^-	OH^-	OH^-	O^{2-}	OH^-	OH^-
OH^-	OH^-	OH^-	OH^-	OH^-	O^{2-}	OH^-
OH^-	OH^-	OH^-	OH^-	OH^-	OH^-	O^{2-}

proton, H^+, is in fact transported from right to left.

Defect electrons are also introduced by a slight deviation from stoicheiometry, *i.e.* any dehydroxylation which might be below the detection limit by analytical means.

The most important difference between the H· and H′ mechanism lies in the fact that the former has a higher activation energy. This can be readily understood on the basis of Figure 7 showing the proton lattice

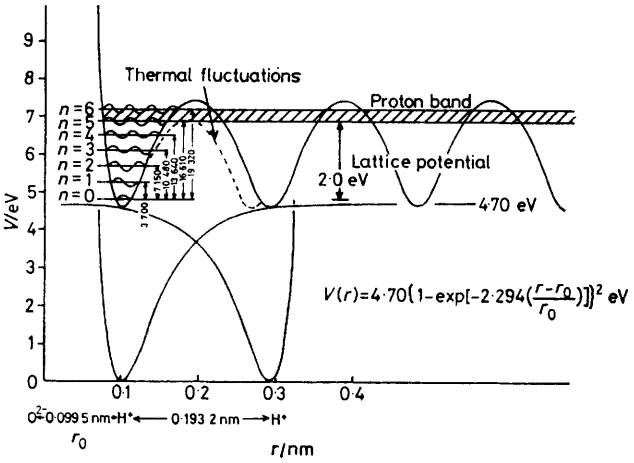

FIGURE 7 Calculated potential-energy curve for the hydroxyl proton in $Mg[OH]_2$ (transition energies, $0 \rightarrow n$, in cm^{-1})

potential of $Mg[OH]_2$ as derived from optical single-crystal data [27] and from proton conductivity measurements.[17-19] In order to become an H· a hydroxyl proton has to be lifted up to the lower edge of the proton conduction band, which requires 2.0 eV in $Mg[OH]_2$. The H′ mechanism, however, requires the activation to one of the intermediate levels only, $n = 2$ in the case of $Mg[OH]_2$, corresponding to 0.8 eV. Both mechanisms will occur simultaneously, if, as inferred by equation (1), the species H′ (O^{2-}) and H· (HOH) are generated thermally in equal number. We call this an intrinsic case.

If we place an intrinsic proton conductor either into an electric field or into a thermal gradient, the two situations arise as depicted in Figure 8. In an electric field the species H· will be drawn from the anode to the cathode which corresponds to a fractional proton flux $i\cdot$ from the anode to the cathode, equation (2) where $n\cdot$, $\mu\cdot$,

$$i\cdot = n\cdot\mu\cdot e \qquad (2)$$

and e are the number, the mobility, and the unit charge of the species H· respectively. At the same time the species H′ will be drawn from the cathode to the anode which, according to the diagram, corresponds in reality to a second proton flux i' from the anode to the cathode, equation (3). The total proton current is then given by

$$i' = n'\mu' e \qquad (3)$$

equation (4). In a temperature gradient both species

$$i = i\cdot + i' \qquad (4)$$

H· and H′ diffuse along the concentration gradient indicated in Figure 8(*b*) by the dotted line. In reality this corresponds to two proton fluxes in opposite directions. Thus, the polarity of the thermopotential set up between the hot and the cold electrode is an indication of the relative mobilities $\mu\cdot/\mu'$. If $\mu\cdot/\mu' > 1$, the cold electrode becomes positively charged (*p*-type behaviour).

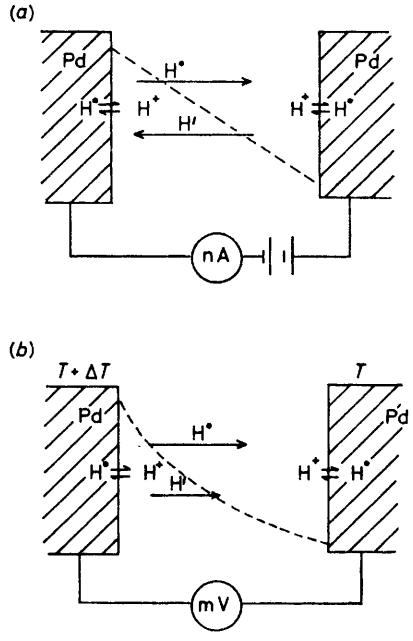

FIGURE 8 Schematic representation of the behaviour of excess proton (H·) and defect protons (H′); (*a*) in an electric field, (*b*) in a temperature gradient

If $\mu\cdot/\mu' < 1$, the cold electrode becomes negatively charged (*n*-type behaviour).

This simple relation holds for the intrinsic case only. If, due to deviations from stoicheiometry, the number of H′ (chemically O^{2-}) exceeds the number of H· (thermally generated protons on some high-lying conduction band), *n*-type behaviour will result, if $n\cdot\mu\cdot/n'\mu' < 1$. Of course, *p*- and *n*-type behaviour can also be caused by other, non-protonic charge carriers such as defect electrons, ions *etc.* In closing this paragraph we would like to recall that proton conductivity can be distinguished from electronic or ionic conductivities by the use of Pd against Au electrodes, because the interface reactions $H^+ + e^- \rightleftharpoons H$ are vital steps in measuring proton currents. If, as in the case of Au, the electrodes are unable to take up hydrogen into solid solution or to inject protons into a proton conductive sample, no steady-state proton current can be transported and measured.

Protonic Thermopotential.—In the case of (OH, F)apatites, using Pd electrodes, the thermopotential was always found to be *p*-type of the order of 10—20 mV K^{-1}. Upon admission of an H_2 pulse, as shown by Figure 6, it changes to the *n*-type direction (0—15 mV K^{-1}), and remains at a plateau which eventually decays after the H_2 has been washed out of the sample chamber. With Au electrodes in N_2 the samples showed the same *p*-type behaviour (10—20 mV K^{-1}) but did not respond to the H_2 pulse. From the positive sign of the thermopotential we can draw the conclusion that the *p*-type characteristic of our (OH, F)apatite under N_2 and with Au electrodes is caused by non-protonic charge carriers, probably defect electrons. Upon admission of the H_2 pulse the dominant charge carriers generated at the Pd electrodes are negatively charged protonic species, defect protons.

Proton Conductivity.—Knowing from the discussion in the preceding section that the admission of a H_2 pulse generates a defect proton flux, we can now turn to the discussion of the remarkably strong d.c. current effects observed with our (OH, F)apatite samples. Since samples in contact with Au electrodes did not show an increase in their conductivity upon admission of an H_2 pulse, the current increase measured with Pd electrodes can only be due to these protonic charge carriers mentioned above, *i.e.* to defect protons.

The very typical and reproducible variations of the proton current as a function of time are shown schematically in Figure 3. We shall not discuss in detail the electrode polarisation effects which are responsible for the complicated time-dependent behaviour of both the conductivity and the thermopotential curves. It suffices to note that immediately after the first proton current maximum (occurring when the partial pressure of H_2 in the sample chamber is high), the current drops to below its value under N_2. This is due to a polarisation of at least one of the electrodes, probably the cathode, by an adsorbed layer of H_2 gas. As the H_2 pulse is washed out of the sample chamber, this insulating gas layer is either desorbed or taken up in solid solution so that the currents can rise slowly to the observed plateau. The plateau corresponds to a situation which can be approximated by a steady state. It breaks down when the partial pressure of H_2 inside the sample chamber drops below a certain value.

By plotting the conductivity values as log σ against T^{-1}, straight lines are obtained. Based on relation (5)

$$\sigma = \sigma_0 \exp(-E/kT) \qquad (5)$$

where σ_0 is the frequency factor, E the activation energy, k the Boltzmann constant, and T the absolute temperature we obtain a constant activation energy, 0.60—0.67 eV, for all apatite samples with 0.15, 35, and 50% F substitution, while the 65, 75, and nearly 100% fluoro-apatite samples give increasingly higher activation energies, 1.1, 1.3, and 1.4 eV respectively. The estimated error is ± 0.1 eV for each case.

Both activation-energy values are below what one would expect for an H· mechanism. They fall into the range of H′ mechanisms.[16-19] This is in agreement with the change of the thermopotentials towards more *n*-type values during H_2 pulses. The magnitude of the activation energies is also in agreement with activation-energy values given for the proton conductivity in ice.[28-30] In

both cases, in ice as well as in the apatite samples studied here, defect protons are the dominant charge carriers.

With increasing F substitution up to 50%, the frequency factor σ_0 increases as shown in Figure 9. This means that, up to 50% F^- in the OH^- chain, the proton transport is enhanced by the presence of F^-. Above 50% however, there is a drastic change; now, with increasing F content, the proton transport is hindered. The point of intersection of the two curves has not yet been determined accurately. It lies around 55—60% F content.

Migratory Mechanism.—Long-range proton transport along an (OH, F) chain through the apatite structure requires. (*a*) a proton exchange between two neighbouring $OH^- \cdots OH^-$ and/or $OH^- \cdots F^-$ ions, and (*b*) a reorientation of individual OH^- and/or FH dipoles. It is quite possible that, when the protons jump from one OH^- to the next, they pass *via* the PO_4^{3-} ions which line the (OH, F) channel. However, this process seems not to be the rate-limiting step of the overall proton transport as evidenced by the distinctly different activation energies for low F content, 0.60—0.67 eV, and for high F content, > 1.1 eV. If the proton were transported only along the PO_4^{3-} ions, one would not expect the pre-exponential factor for the proton conductivity to increase exponentially with increasing F^- content, nor should there be such a pronounced and sudden increase of the activation energy when the F^- content increases beyond 50%.

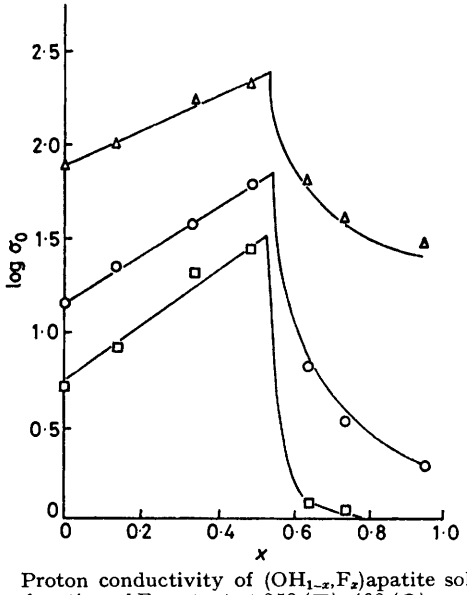

FIGURE 9 Proton conductivity of (OH_{1-x},F_x)apatite solid solutions as a function of F content at 350 (□), 400 (○), and 500 °C (△)

Disregarding the as yet unknown exact pathway of the proton, we can formulate a defect proton mechanism as illustrated in Figure 10 for (A), pure OH^- chains; (B), $(OH, F)^-$ chains containing a single F^- ion only; and (C), fluorine-rich $(OH, F)^-$ chains containing three or more F^- ions in a row. For case (A) the rate-limiting process for the proton transport may either be the dipole reorientation (steps 1 and 2) or the proton shift (steps 2 and 3).

The conductivity results indicate that single F^- ions, if incorporated into the OH^- chain, case (B), do not alter the overall activation energy but make the proton transport faster. This is possible only if the activation energies of the steps 3—6 are lowered with respect to case (A) so that the partial proton transport mechanism past the F^- ions is speeded up. Here PO_4^{3-} ions may play an important part.

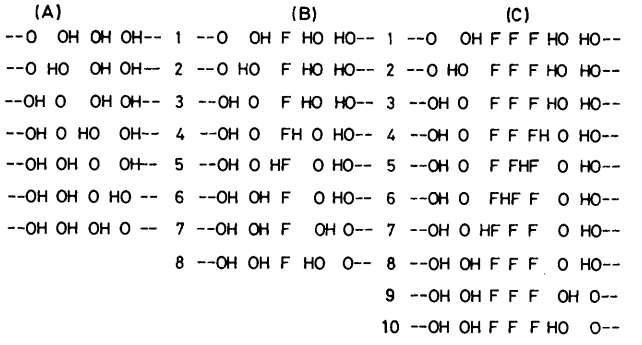

FIGURE 10 Schematic representation of proton migration along anionic chain parallel to *c* axis. (A) Pure hydroxyapatite, (B) OH chain containing few F^- ions, (C) OH chain containing an excess of F^- ions

On the contrary, in case (C), configurations occur with two, three, or more F^- ions in a row. According to the conductivity results, they introduce high activation energies for the proton transport past them. Probably the enantiomorphic configurations $(FFHF)^{2-} \rightleftharpoons (FHFF)^{2-}$ strongly retain the protons; the longer the F sections become, the higher is the activation energy and the lower the frequency factor. Alternatively the proton may become locked at PO_4^{3-} ions neighbouring such longer F sequences.

Conclusions.—The combination of protonic conductivity measurements reported in this paper indicates that (*a*) proton conductivity occurs along OH^- chains in pure hydroxyapatite, (*b*) proton conductance is enhanced by incorporation of F^- up to *ca.* 50 mol % in $(OH, F)^-$ apatites, and (*c*) fluorine-rich sections in the transport chain effectively lower the proton conductance. The improved understanding of the proton conductivity mechanism along the linear (OH, F) chains in the apatite structure may be helpful for aspects of caries research.

Financial support from the Deutsche Forschungsgemeinschaft, Bonn, is acknowledged. One of us (G. C. M.) is grateful for leave of absence granted by the Fertilizer Corporation of India, Research and Development Division, Bihar, India, and a grant from the Heinrich-Hertz-Stiftung Düsseldorf.

[0/621 *Received*, 28*th April*, 1980]

REFERENCES

[1] M. I. Kay, R. A. Young, and A. S. Posner, *Nature (London)*, 1964, **204**, 1050.
[2] J. S. Prener, *J. Electrochem. Soc.*, 1967, **114**, 77.
[3] W. Eysel and D. M. Roy, *J. Cryst. Growth*, 1973, **20**, 245.

[4] T. S. B. Narasaraju, R. P. Singh, and V. L. N. Rao, *J. Inorg. Nucl. Chem.*, 1972, **34**, 2072.
[5] D. McConnell, ' Apatite,' Springer, New York, 1973.
[6] R. A. Young, W. Vanderlugt, and J. C. Elliot, *Nature (London)*, 1969, **223**, 729.
[7] D. M. Adams and I. R. Gardner, *J. Chem. Soc., Dalton Trans.*, 1974, 1505.
[8] B. O. Fowler, *Inorg. Chem.*, 1974, **13**, 194.
[9] N. W. Cant, J. A. S. Bett, and W. H. Hall, *Spectrochim Acta, Part A*, 1971, **27**, 425.
[10] F. Freund and R. M. Knobel, *J. Chem. Soc., Dalton Trans.*, 1977, 1136.
[11] H. Kistenmacher, H. Popkie, and E. Clementi, *J. Chem. Phys.* 1972, **11**, 5842; *ibid.*, 1973, **11**, 5627.
[12] K. Nakamoto, M. Margoshes, and R. E. Rundle, *J. Am. Chem. Soc.*, 1955, **77**, 6480.
[13] B. S. H. Royce, *J. Phys. (Paris), Colloq.*, 1973, **11–12**, C327.
[14] H. Den Hartog, D. O. Welch, and B. S. H. Royce, *Phys. Status Solidi B*, 1972, **53**, 201.
[15] J. Arends, B. S. H. Royce, D. Welch, and R. Smoluchowski, unpublished work.
[16] F. Freund and R. Hösen, *Ber. Bunsenges. Phys. Chem.*, 1977, **81**, 39.
[17] F. Freund and H. Wengeler, *Ber. Bunsenges. Phys. Chem.*, 1980, **84**, 866.
[18] H. Wengeler, R. Martens, and F. Freund, *Ber. Bunsenges. Phys. Chem.*, 1980, **84**, 873.
[19] F. Freund, H. Wengeler, and R. Martens *J. Chim. Phys. Phys.-Chim. Biol.*, 1980, **77**, 837.
[20] J. F. Volker, *Proc. Soc. Exp. Biol. Med.*, 1939, **42**, 725.
[21] G. S. Ingram, *Caries Res.*, 1973, **7**, 315.
[22] O. Baker-Dirks, *Caries Res. Suppl.*, 1974, **8**, 215.
[23] F. Freund, *Inorg. Nucl. Chem. Lett.*, 1977, **13**, 57.
[24] C. Rey, J. C. Trombe, and G. Montel, *J. Inorg. Nucl. Chem.*, 1978, **40**, 27.
[25] J. C. Trombe and G. Montel, *J. Inorg. Nucl. Chem.*, 1978, **40**, 15.
[26] R. Hösen, Ph.D. Thesis, University of Köln, 1979.
[27] R. Martens and F. Freund, *Phys. Status. Solidi A*, 1976, **37**, 97.
[28] B. Bullemer, I. Eisele, H. Engelhardt, N. Riehland, and P. Seige, *Solid State Commun.*, 1968, **6**, 663.
[29] R. S. Bradley, *Trans. Faraday Soc.*, 1957, **53**, 687.
[30] M. A. Maidique, A. von Hippel, and W. B. Westphal, *J. Chem. Phys.*, 1971, **54**, 150.